AIP Advances

Dimensionality-induced insulator-metal crossover in layered nickelates La n+1Ni n O2n+2 (n = 2, 3, and ∞)

Ting Liu, Hua Wu, Ting Jia, Xiaoli Zhang, Zhi Zeng, H. Q. Lin, and X. G. Li

Citation: AIP Advances **4**, 047132 (2014); doi: 10.1063/1.4873537
View online: http://dx.doi.org/10.1063/1.4873537
View Table of Contents: http://scitation.aip.org/content/aip/journal/adva/4/4?ver=pdfcov
Published by the AIP Publishing

AIP ADVANCES **4**, 047132 (2014)

Dimensionality-induced insulator-metal crossover in layered nickelates $La_{n+1}Ni_nO_{2n+2}$ ($n = 2$, 3, and ∞)

Ting Liu,[1] Hua Wu,[2,a] Ting Jia,[1] Xiaoli Zhang,[1] Zhi Zeng,[1,3,b] H. Q. Lin,[4] and X. G. Li[3]

[1]*Key Laboratory of Materials Physics, Institute of Solid State Physics, Chinese Academy of Sciences, Hefei 230031, China*
[2]*Laboratory for Computational Physical Sciences (MOE), State Key Laboratory of Surface Physics, and Department of physics, Fudan University, Shanghai 200433, China*
[3]*Hefei National Laboratory for Physical Sciences at Microscale, Department of Physics, University of Science and Technology of China, Hefei 230026, China*
[4]*Beijing Computational Science Research Center, Beijing 100084, China*

(Received 8 February 2014; accepted 15 April 2014; published online 24 April 2014)

Low-valence layered nickelates are a structural analog to the superconducting cuprates and possess interesting properties. In this work, we have systematically studied the electronic structure of $La_{n+1}Ni_nO_{2n+2}$ using first-principles calculations. Our results reveal that the Ni-3*d* $3z^2 - r^2$ orbital state is active and evolves from discrete molecular levels to a continuous solid band and its filling varies as the dimensionality (or *n*) increases. The two-dimensional (2D) $La_3Ni_2O_6$ and $La_4Ni_3O_8$ are thus found to have a molecular insulating state. In contrast, the 3D $LaNiO_2$ is metallic and its $3z^2 - r^2$ band surprisingly becomes 3D due to the Ni-La hybridization, and the La-5*d* *xy* orbital also forms a 2D metallic band. Therefore, $La_{n+1}Ni_nO_{2n+2}$ is a dimensionality-controlled insulator-metal crossover system. [http://dx.doi.org/10.1063/1.4873537]

I. INTRODUCTION

Insulator-metal transition (IMT) is an interesting property of transition metal oxides. It is scientifically important for the physics behind it, and it may also be explored for technological applications.[1] IMT is often driven by a competition between electron correlations and band effects. Moreover, very often the charge, spin, orbital, and lattice degrees of freedom get involved, making IMT to be a complex issue.[2] As well known, dimensionality (D) is another important factor to tune materials properties, and dimensionality controlled IMT has often been observed in films and superlattices.[3–7] $LaNiO_3$-based superlattice undergoes a metal-insulator transition when the thickness of $LaNiO_3$ is reduced to only a few unit cells.[7] Moreover, the dimensionality-induced IMT occurs in bulk Ruddlesden-Popper series $Sr_{n+1}Ir_nO_{3n+1}$ ($n = 1$, 2, and ∞).[8] The bulk T′-type nickelates $La_{n+1}Ni_nO_{2n+2}$ ($n = 2$, 3, and ∞)[9–21] with infinite NiO_2 square planes seem to be another candidate for the dimensionality-controlled IMT. They contain bilayer, trilayer and infinite-layer of NiO_2 planes for $La_3Ni_2O_6$ ($n = 2$), $La_4Ni_3O_8$ ($n = 3$) and $LaNiO_2$ ($n = \infty$), respectively, as shown in Fig. 1. Owing to the sandwiching LaO fluorite blocks, the inter-bilayer (inter-trilayer) coupling is very weak and therefore $La_3Ni_2O_6$ ($La_4Ni_3O_8$) shows 2D features. In contrast, $LaNiO_2$ is expected to be 3D. Thus, the dimensionality of the electron system is changed from 2D to 3D as the number of NiO_2 planes (*n*) increases. Moreover, transport and magnetic measurements have shown that $La_3Ni_2O_6$ is a highly paramagnetic insulator[10] with antiferromagnetic (AFM) spin fluctuations below 5 K[21] and $La_4Ni_3O_8$ is an AFM insulator below 105 K,[13] whereas $LaNiO_2$ exhibits a correlated metallic

[a]Electronic mail: wuh@fudan.edu.cn
[b]Electronic mail: zzeng@theory.issp.ac.cn

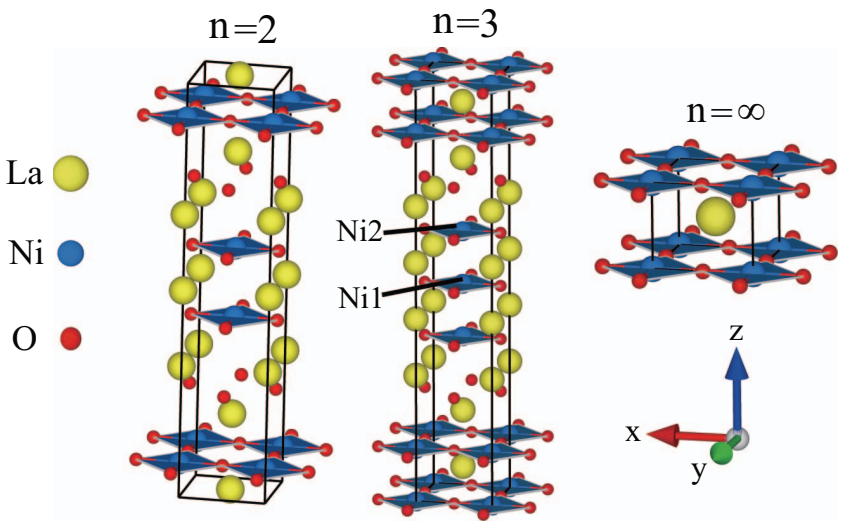

FIG. 1. The crystal structure of $n = 2$ ($La_3Ni_2O_6$), 3 ($La_4Ni_3O_8$) and ∞ ($LaNiO_2$) members. The corner-sharing NiO_2 square planes are highlighted in blue with Ni atoms at the centers. La atoms are represented by yellow (big) spheres and O atoms by red (small) spheres. For $n = 2$ member, interlayer $d_{Ni-Ni} = 3.19$ Å, intralayer $d_{Ni-O} = 1.9844$ Å; for $n = 3$ member, interlayer $d_{Ni1-Ni2} = 3.25$ Å, intralayer $d_{Ni1-O} = 1.9817$ Å, $d_{Ni2-O} = 1.9819$ Å; for $n = \infty$ member, interlayer $d_{Ni-Ni} = 3.375$ Å, intralayer $d_{Ni-O} = 1.9795$ Å.

behavior with short-ranged AFM ordering.[16] So $La_{n+1}Ni_nO_{2n+2}$, with $n = 2$, 3, and ∞, have an insulator-metal crossover. However, a theoretical understanding of those diverse properties is far from being satisfactory. Poltavets *et al.*[10,13] and Sarkar *et al.*[12] obtained a correlated metallic ground state for both $La_3Ni_2O_6$ and $La_4Ni_3O_8$ from first-principles calculations. In contrast, Pardo and Pickett[11,15] and Liu *et al.*[19] found a molecular correlated insulating ground state, which is similar to a partially charge-disproportioned insulating state proposed by Wu.[20] Anisimov *et al.*[18] reported that $LaNiO_2$ is an AFM insulator similar to $CaCuO_2$ (Ref. 22), but it was suggested to be nonmagnetic (NM) and probably metal by Lee and Pickett.[17] Apparently, those ground-state solutions are contradictory. We are therefore motivated to carry out a systematic study on $La_{n+1}Ni_nO_{2n+2}$ and to probe a possible impact of the dimensionality on their electronic structures.

In this paper, we have performed electron-correlation corrected density-functional calculations for $La_{n+1}Ni_nO_{2n+2}$ ($n = 2$, 3, and ∞). The insulator-metal crossover in $La_{n+1}Ni_nO_{2n+2}$ is found to be induced by dimensionality. When the dimensionality (or n) increases, the active $3z^2 - r^2$ orbital state is gradually developed from the discrete molecular levels for 2D $La_3Ni_2O_6$ and $La_4Ni_3O_8$ to continuous solid band for 3D $LaNiO_2$. Meanwhile, the filling of down-spin $3z^2 - r^2$ orbital varies. Thus, a molecular insulating state is formed in 2D $La_3Ni_2O_6$ and $La_4Ni_3O_8$, while a metallic state is found for 3D $LaNiO_2$. Our results also indicate that the metallic state of $LaNiO_2$ is induced by the Ni-3*d*/La-5*d* hybridization, which gives rise to the unusual 3D Ni-3*d* $3z^2 - r^2$ metallic band and the 2D La-5*d* *xy* metallic band.

II. COMPUTATIONAL DETAILS

Our calculations were performed using the standard full-potential linearized augmented plane wave code WIEN2k[23] within density functional theory. We have first done structural optimization and find that the equilibrium volumes are slightly different from the experimental ones by 0.6%, 0.75% and −0.3% at most, and that the Ni-Ni and Ni-O distances of the most concern change by 0.2%, 0.24% and −0.1% at most for $La_3Ni_2O_6$, $La_4Ni_3O_8$ and $LaNiO_2$, respectively. Therefore, the experimental lattice parameters (see Table I) are well reproduced by our calculations. We present below the calculated results using those experimental structure parameters. The muffin-tin sphere radii were chosen to be 2.35, 1.97 and 1.75 bohr for La, Ni and O atoms, respectively. The cutoff

TABLE I. The lattice constants *a*, *c* (Å) and atomic coordinates for $La_3Ni_2O_6$ (Space group: *I*4/*mmm*, Ref. 9), $La_4Ni_3O_8$ (Space group: *I*4/*mmm*, Ref. 13) and $LaNiO_2$ (Space group: *P*4/*mmm*, Ref. 16), respectively.

	$La_3Ni_2O_6$	$La_4Ni_3O_8$	$LaNiO_2$
a	3.9686	3.9633	3.9592
c	19.3154	26.0373	3.3745
La1	(0,0,0.5)	(0,0,0.4333)	(0.5,0.5,0.5)
La2	(0,0,0.3170)	(0,0,0.2996)	
Ni1	(0,0,0.0826)	(0,0,0)	(0,0,0)
Ni2		(0,0,0.1248)	
O1	(0,0.5,0.25)	(0,0.5,0)	(0.5,0,0)
O2	(0,0.5,0.0838)	(0,0.5,0.25)	
O3		(0,0.5,0.1261)	

parameter $R_{mt}K_{max}$ was set to 7.0 (the smallest muffin-tin radius multiplied by the maximal K vector which truncates the plane-wave expansion in the basis set) and G_{max} was set to 12 for the charge density Fourier expansion. Here, 500 and 1000 *k*-points were used over the first Brillouin zone for $La_3Ni_2O_6$ and $LaNiO_2$, respectively. Self-consistency was considered to be achieved when the total energy difference between succeeding iterations is less than 10^{-5} Ry/unit cell. The generalized gradient approximation (GGA) by Perdew, Burk, and Ernzerhof[24] was employed for the exchange-correlation potential. To properly describe the strong electron correlation associated with the Ni 3*d* states, the GGA+*U* scheme in the so-called fully localized limit[25] was used, where $U_{eff} = U\text{-}J$ (*U* and *J* are on-site Coulomb and exchange interaction, respectively) was used instead of *U*.[26] The parameters U_{eff} have been investigated by examining the evolution of the total energy of different spin configurations with variation of U_{eff}. To clarify the magnetic structure, $\sqrt{2} \times \sqrt{2} \times 1$ and $\sqrt{2} \times \sqrt{2} \times 2$ supercell calculations were performed for $La_3Ni_2O_6$ and $LaNiO_2$, respectively, with four possible spin configurations: C-AFM (AFM within layers, FM between layers), A-AFM (FM within layers, AFM between layers), G-AFM (AFM within layers and AFM between layers) and FM spin configurations.

III. RESULTS AND DISCUSSIONS

In $La_{n+1}Ni_nO_{2n+2}$ compounds, the electron correlation values may be one of causes that the calculated ground state remains controversial.[19,27] Therefore, it is necessary to investigate the proper electron correlation values of Ni 3*d* for $La_{n+1}Ni_nO_{2n+2}$. To choose the reasonable electron correlation values, we examine the evolution of the total energy of different spin configurations with variation of *U*. The ground state of $La_3Ni_2O_6$ is a function of *U*, as shown in Fig. 2(a). $La_3Ni_2O_6$ exhibits the metallic ground state by using small electron correlation value ($U = 0$-4 eV), which is inconsistent with the experimental data.[10,21] The experimentally observed insulating ground state of $La_3Ni_2O_6$ is obtained when $U = 4.3$-6 eV. For $La_4Ni_3O_8$, the metallic state is most stable if $0 \leq U \leq 4.3$ eV, whereas the insulating state is the ground state when $5 \leq U \leq 6$ eV[19] (see Fig. 2(b)). Thus, $U = 5$-6 eV[19] is the proper Ni 3*d* electron correlation values for $La_4Ni_3O_8$. Moreover, $LaNiO_2$ exhibits observed correlated metallic behavior[16] and no significant change to electronic structure, as changing *U* from 3 to 6 eV (see Fig. 2(c)). Hence, the $U = 5$ eV is the appropriate Ni 3*d* electron correlation value in $La_{n+1}Ni_nO_{2n+2}$ compounds.

The relative energies of various spin configurations are studied within GGA+*U* ($U = 5$ eV). For $La_3Ni_2O_6$, as shown in Table II, both FM and A-AFM states exhibit a metallic feature which disagrees with the experimental data. Both C-AFM and G-AFM states exhibit experimentally observed insulating behavior, but the C-AFM state is more stable than the G-AFM state in energy by 218 meV/Ni. Therefore, the C-AFM state is the ground state which is consistent with the results reported by Pardo and Pickett.[11] No long-ranged magnetic ordering was found[10] in $La_3Ni_2O_6$, but the nuclear magnetic resonance (NMR) data revealed the presence of AFM spin fluctuations at low temperature.[21] It suggests a short-ranged AFM ordering. For $La_4Ni_3O_8$, the energy of C-AFM state

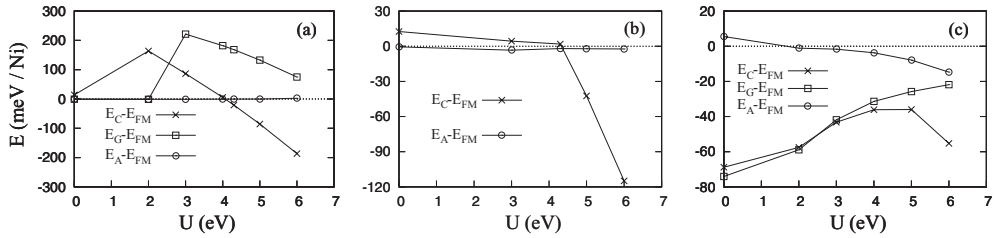

FIG. 2. Relative total energy of different magnetic states as a function of U for (a) $La_3Ni_2O_6$, (b) $La_4Ni_3O_8$ and (c) $LaNiO_2$.

TABLE II. The total energy ΔE (meV/ Ni) relative to the lowest-energy state, the magnetic moment M_s (μ_B) of Ni, band gap E_g (eV) for different magnetic configurations within GGA+U ($U_{eff} = 5$ eV). In the calculations, the magnetic moments are assumed to be along the crystallographic c-axis. Actually they are rotationally free in the space without the spin-orbit coupling effect. "–" denotes metal. The data of $La_4Ni_3O_8$ are from Ref. 19

		FM	*A*-AFM	*C*-AFM	*G*-AFM
$La_3Ni_2O_6$	ΔE	86	85	0	218
	M_s	0.69/0.60	±0.6	±1.43	0.92/-1.54
	E_g	–	–	1.0	1.4
$La_4Ni_3O_8$	ΔE	42.32	40.16	0	
	M_s	0.79/0.77	±0.8	1.44/1.29	
	E_g	–	–	0.7	
$LaNiO_2$	ΔE	36	28	0	10
	M_s	1	±1.08	±1.13	±1.06
	E_g	–	–	–	–

is lower than that of FM and A-AFM states by about 80 meV/Ni[19] (see Table II), and consequently the C-AFM state is the ground state. And similarly, the C-AFM state is most stable for $LaNiO_2$, which is lower in energy than FM, A-AFM and G-AFM states by 36, 28 and 10 meV/Ni, respectively. Neutron diffraction and spin susceptibility measurements indicated that $LaNiO_2$ shows short-ranged AFM ordering.[16] Lee and Pickett[17] have suggested that $LaNiO_2$ may be a NM metal. However, our obtained NM state is less stable than the C-AFM state by 70 meV/Ni. Consequently, the C-AFM state is preferred for $La_{n+1}Ni_nO_{2n+2}$ compounds, although AFM ordering is a marginal occurrence and only short-ranged AFM ordering[28] exits in $La_3Ni_2O_6$ and $LaNiO_2$.

$La_3Ni_2O_6$ ($n = 2$) exhibits insulating character with a band gap of 1 eV (see Fig. 3(a)). The states driven by Ni 3d-O 2p hybridized orbitals mainly distribute from −6 to −0.2 eV and from 3 to 5 eV, and the states near the Fermi level are mainly driven by Ni 3d orbitals. According to a simple electron count, the Ni ions have 1.5+ oxidation state with charge $d^{8.5}$. From Fig. 3(a), we can see that the Ni ions hold the high-spin state (S = 3/4, $M_s = 1.5\ \mu_B$), which is consistent with the previous solution by Pardo and Pickett.[11] The t_{2g} orbitals of Ni-3d are completely occupied, distributing from –5.6 eV to –0.7 eV (not shown here). The up-spin $x^2 - y^2$ orbital is fully occupied, while the down-spin $x^2 - y^2$ orbital is empty, showing the large exchange splitting (due to the electron correlation rather than Hund exchange). The up-spin $3z^2 - r^2$ orbital is fully filled, distributing from –6 eV to –3 eV. The down-spin $3z^2 - r^2$ orbital is half filled, contributing 0.5 μ_B to Ni spin moment. Particularly, its filled and unfilled bands correspond to highly localized molecular levels.

$La_4Ni_3O_8$ ($n = 3$) also shows insulating character with a band gap of 0.7 eV[19] (see Fig. 3(b)). It has a similar density of states (DOS) except that down-spin $3z^2 - r^2$ orbital is two-thirds filled, as shown in Fig. 3(b). Its unfilled band is separated from filled bands by band gap of 0.7 eV and all of them are quite localized as in $La_3Ni_2O_6$. The oxidation state of the Ni ions is 1.33+ with charge $d^{8.67}$ and the Ni ions are in high-spin state (S = 2/3, $M_s = 1.33\ \mu_B$).[15,19] The unfilled down-spin $x^2 - y^2$ orbital contributes 1 μ_B to Ni spin moment and the two-thirds filled down-spin $3z^2 - r^2$ orbital contributes 0.33 μ_B.[15]

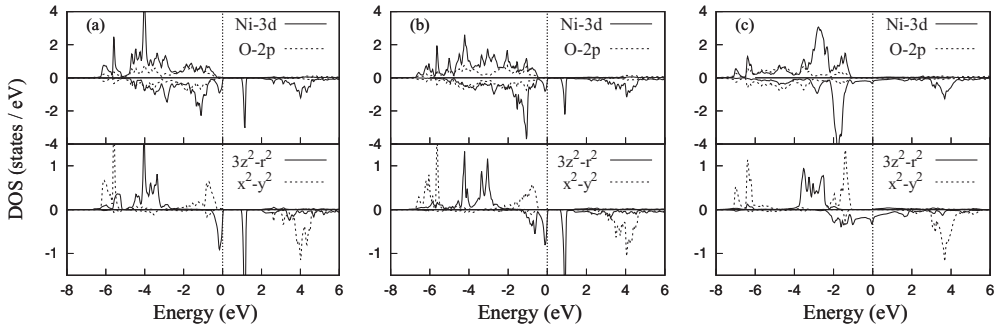

FIG. 3. The Ni-3*d* orbital-resolved partial density of states (DOS) and O-2*p* DOS obtained from GGA+U (U = 5 eV) in C-AFM ground state for (a) $La_3Ni_2O_6$, (b) $La_4Ni_3O_8$, and (c) $LaNiO_2$.

$LaNiO_2$ ($n = \infty$) exhibits a metallic character. The DOS crossing the Fermi level has a large contribution from $3z^2 - r^2$ orbital and a small contribution from O-2*p* orbitals, as shown in Fig. 3(c). $LaNiO_2$ has Ni^+:d^9 cations, the spin moment is increased to 1.13 μ_B because of the hybridization between the $3z^2 - r^2$ and other empty orbitals. Like $La_3Ni_2O_6$ and $La_4Ni_3O_8$, the t_{2g} orbitals of Ni-3*d* are completely occupied, distributing from –6.1 eV to –1.3 eV. The up-spin $x^2 - y^2$ orbital is filled, while the down-spin $x^2 - y^2$ orbital is unfilled, respectively lying 1.1 eV below and 3 eV above the Fermi level. In contrast to $La_3Ni_2O_6$ and $La_4Ni_3O_8$, the down-spin $3z^2 - r^2$ orbital now forms a broad metallic band crossing the Fermi level due to the Ni-La hybridization (see below). The Ni-3*d* and La-5*d* hybridized orbitals were also found in Ref. 17.

Next, we seek the origin of insulator-metal crossover upon increasing the n from $n = 2$ ($La_3Ni_2O_6$) and $n = 3$ ($La_4Ni_3O_8$) to $n = \infty$ ($LaNiO_2$) using the above results. The t_{2g} and $x^2 - y^2$ orbitals of Ni-3*d* in these compounds are away from the Fermi level and do not contribute to the conductivity. In addition, as its exchange splitting is large, the top of the up-spin $3z^2 - r^2$ band is lower than the bottom of down-spin $3z^2 - r^2$ band (see Fig. 3). Therefore, the state determining their conductivity is the partially filled down-spin $3z^2 - r^2$ orbital which is active in the vicinity of the Fermi level. The down-spin $3z^2 - r^2$ orbital evolves from molecular level states to a solid band state and its filling varies from 1/2 to 2/3 and then to 1, when n or the dimensionality increases.

When $n = 2$, $La_3Ni_2O_6$ has NiO_2 bilayers separated by LaO fluorite blocks, thereby showing 2D features see Fig. 1. This strong structural confinement makes the NiO_2 bilayer of $La_3Ni_2O_6$ form a molecular dimer via the down-spin $3z^2 - r^2$ orbital along the z-axis. The down-spin $3z^2 - r^2$ orbital within dimer is split into discrete bonding (*b*) and antibonding (*ab*) levels (see Fig. 4(a)). These molecular levels are highly localized with their level-width being less than 0.65 eV (see Fig. 3(a)) as a consequence of the limited-dimensionality. This molecular picture can be understood by a simple two-site tight-binding (TB) model. According to the TB model, the energy separation between bonding and antibonding levels is $2t_2$ within dimer (t_2 is the interlayer hopping in $La_3Ni_2O_6$). From Fig. 3(a), we can see that the bonding and antibonding levels of $La_3Ni_2O_6$ are located at –0.2 and 1.1 eV, respectively. Then, we can estimate the hoppings t_2 to be 0.65 eV. It is the bonding-antibonding splitting which determines the insulating gap, see Figs. 3(a) and 4(a).

When $n = 3$, $La_4Ni_3O_8$ has NiO_2 trilayers separated by LaO fluorite blocks, thereby showing also 2D features. This structural confinement makes NiO_2 trilayer of $La_4Ni_3O_8$ form a molecular trimer via the interlayer interaction mediated by the down-spin $3z^2 - r^2$ orbital.[15] According to the three-site TB model, the down-spin $3z^2 - r^2$ orbital within dimer is split into discrete bonding (*b*), nonbonding (*nb*), antibonding (*ab*) levels and the bonding-antibonding splitting value is $2\sqrt{2}t_3$ (t_3 is the hopping in $La_4Ni_3O_8$)(see Fig. 4(b)). The bonding, nonbonding and antibonding levels of $La_4Ni_3O_8$ are located at –1, –0.1 and 0.8 eV (see Fig. 3(b)), respectively, thus the hoppings t_3 is estimated to be 0.64 eV. t_3 is slightly smaller than t_2, which originates from the tiny difference in structural details (The Ni-Ni interlayer distance is 3.19 Å for $La_3Ni_2O_6$ and 3.25 Å for $La_4Ni_3O_8$). These molecular levels are also quite localized with their level-width being less than 0.75 eV (see Fig. 3(b)). Compared with $La_3Ni_2O_6$, the bonding-antibonding splitting is enhanced and the third

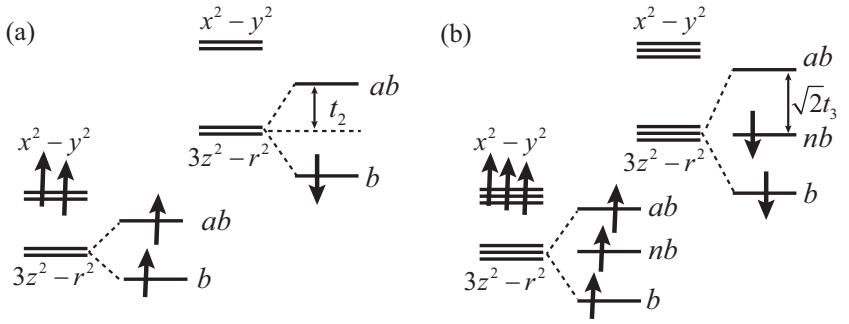

FIG. 4. The molecular level diagram for (a) $La_3Ni_2O_6$ and (b) $La_4Ni_3O_8$. Only the e_g states are depicted, with the bonding (*b*), antibonding (*ab*), and nonbonding (*nb*) levels. t_2 (the interlayer hopping in $La_3Ni_2O_6$) and t_3 (the interlayer hopping in $La_4Ni_3O_8$) are about 0.65 eV and 0.64 eV, respectively.

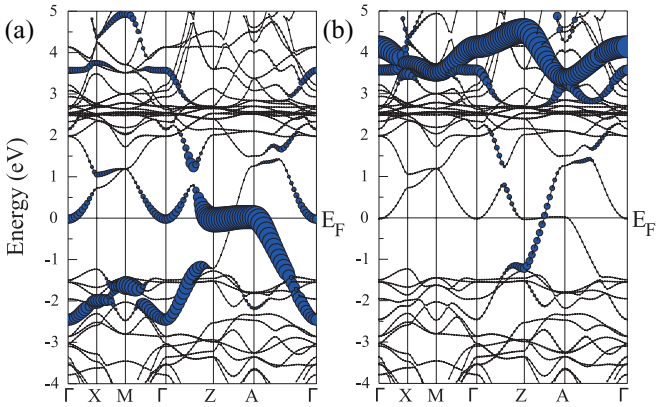

FIG. 5. The minority-spin band structure of $LaNiO_2$ with the highlighted Ni-3*d* $3z^2$-r^2 orbital in (a) and La-5*d* *xy* orbital in (b). In (b) the metallic band along Z-A direction is mainly due to the La-5*d* *xy* state.

molecular level is inserted, due to the additional NiO_2 layer in $La_4Ni_3O_8$. Thus, a smaller band gap is formed between the filled nonbonding level and the unfilled antibonding one for 2/3-filled down-spin $3z^2 - r^2$ orbital.

When $n = \infty$, $LaNiO_2$ shows 3D features due to the absent of LaO confining block, therefore the $3z^2 - r^2$ orbital expands to the continuous band. On the one hand, $LaNiO_2$ with Ni^+ (d^9) may be expected to have a completely occupied down-spin $3z^2 - r^2$ orbital, and thus to have an insulating behavior. However, the down-spin $3z^2 - r^2$ orbital actually forms a broad metallic band and the La-5*d* bands also cross Fermi level, as shown in Fig. 5. On the other hand, the bandwidth of down-spin $3z^2 - r^2$ orbital would be $4t$ if it is the normal 1D type along the *z*-axis, according to the TB model. As the Ni-Ni interlayer distance of 3.375 Å in $LaNiO_2$ is larger than that in $La_4Ni_3O_8$ (3.25 Å), the hopping parameter t in the former would be smaller than t_3 in the latter. That is to say, the bandwidth of down-spin $3z^2 - r^2$ orbital in $LaNiO_2$ would be smaller than $4t_3$ if the $3z^2 - r^2$ is 1D as usual. However, the actual down-spin $3z^2 - r^2$ bandwidth of more than 4 eV in $LaNiO_2$ (see Figs. 3(c) and 5(a)) is much larger than $4t_3$ (about 2.6 eV). This suggests that besides the interlayer Ni-Ni hopping, the Ni-La hybridization greatly enhances the $3z^2 - r^2$ bandwidth and results in a metallic state. The higher on-site energy of Ni^+ 3*d* orbital, compared with $Ni^{1.5+}$ and $Ni^{1.33+}$, reduces the energy separation between Ni-3*d* and diffusive La-5*d* bands, thereby enhancing the hybridization between them.[17] Thus, a finite electron transfer from Ni-3*d* $3z^2 - r^2$ to La-5*d* *xy* results in a metallic state. Owing to the Ni 3*d*-La5*d* hybridization, the $3z^2 - r^2$ band has a large dispersion along A-Γ direction (see Fig. 5(a)), showing a remarkable 3D character but not the normal 1D. Moreover, La *xy* forms a 2D metallic band along the Z-A direction, see Fig. 5(b).

IV. CONCLUSIONS

In summary, we have investigated the electronic structure of low-valence layered nickelates $La_{n+1}Ni_nO_{2n+2}$ using first-principle calculations. We find that $La_{n+1}Ni_nO_{2n+2}$ is a dimensionality-controlled insulator-metal crossover system. When the dimensionality (or n) increases, the active $3z^2 - r^2$ orbital state evolves from molecular levels to a solid band and its corresponding filling is increased. The $3z^2 - r^2$ orbital split into bonding and antibonding levels for 2D $La_3Ni_2O_6$ and its corresponding 1/2-filling lead to a molecular insulating state with large band gap. For 2D $La_4Ni_3O_8$, the $3z^2 - r^2$ orbital split into bonding, nonbonding and antibonding levels and its corresponding 2/3-filling lead to a molecular insulating state with relatively small band gap. For 3D $LaNiO_2$, however, the $3z^2 - r^2$ orbital is expanded into a continuous metallic band. Owing to the Ni-3*d* and La-5*d* hybridization and a finite charge transfer, the $3z^2 - r^2$ orbital shows a surprising 3D behavior, and La-5*d* *xy* orbital forms a 2D metallic band. The present study clarifies the important role of the dimensionality and the inter-orbital hybridization in determining the electronic structure of insulator-metal crossover system $La_{n+1}Ni_nO_{2n+2}$.

ACKNOWLEDGMENTS

This work was supported by the NSF of China under Grant Nos. 11204309, 11204310 and U1230202(NSAF), the special Funds for Major State Basic Research Project of China (973) under Grant No. 2012CB933702, Heifei Center for Physical Science and Technology under Grant No. 2012FXZY004. The calculations were performed in Center for Computational Science of CASHIPS and on the ScGrid of Supercomputing Center, Computer Network Information Center of CAS. H. Wu is supported by the NSF of China (Grant No. 11274070), by ShuGuang Program of Shanghai (Grant No. 12SG06), and by PuJiang Program of Shanghai (Grant No. 12PJ1401000).

[1] M. Imada, A. Fujimori, and Y. Tokura, Rev. Mod. Phys. **70**, 1039–1263 (1998).
[2] E. Dagotto, Science **309**, 257 (2005).
[3] K. Yoshimatsu, T. Okabe, H. Kumigashira, S. Okamoto, S. Aizaki, A. Fujimori, and M. Oshima, Phys. Rev. Lett. **104**, 147601 (2010).
[4] K. Yoshimatsu, K. Horiba, H. Kumigashira, T. Yoshida, A. Fujimori, and M. Oshima, Science **333**, 319 (2011).
[5] J. Liu, S. Okamoto, M. van Veenendaal, M. Kareev, B. Gray, P. Ryan, J. W. Freeland, and J. Chakhalian, Phys. Rev. B **83**, 161102 (2011).
[6] A. V. Boris, Y. Matiks, E. Benckiser, A. Frano, P. Popovich, V. Hinkov, P. Wochner, M. Castro-Colin, E. Detemple, V. K. Malik, C. Bernhard, T. Prokscha, A. Suter, Z. Salman, E. Morenzoni, G. Cristiani, H.-U. Habermeier, and B. Keimer, Science **332**, 937 (2011).
[7] S. J. May, T. S. Santos, and A. Bhattacharya, Phys. Rev. B **79**, 115127 (2009).
[8] S. J. Moon, H. Jin, K. W. Kim, W. S. Choi, Y. S. Lee, J. Yu, G. Cao, A. Sumi, H. Funakubo, C. Bernhard, and T. W. Noh, Phys. Rev. Lett. **101**, 226402 (2008).
[9] V. V. Poltaverts, K. A. Lokshin, S. Dikmen, M. Croft, T. Egami, and M. Greeblatt, J. Am. Chem. Soc. **128**, 9050 (2006).
[10] V. V. Poltavets, M. Greenblatt, G. H. Fecher, and C. Felser, Phys. Rev. Lett. **102**, 046405 (2009).
[11] V. Pardo and W. E. Pickett, Phys. Rev. B **83**, 245128 (2011).
[12] S. Sarkar, I. Dasgupta, M. Greenblatt, and T. Saha-Dasgupta, Phys. Rev. B **84**, 180411 (2011).
[13] V. V. Poltavets, K. A. Lokshin, A. H. Nevidomskyy, M. Croft, T. A. Tyson, J. Hadermann, G. Van Tendeloo, T. Egami, G. Kotliar, N. ApRoberts-Warren, A. P. Dioguardi, N. J. Curro, and M. Greenblatt, Phys. Rev. Lett. **104**, 206403 (2010).
[14] N. ApRoberts-Warren, A. P. Dioguardi, V. V. Poltavets, M. Greenblatt, P. Klavins, and N. J. Curro, Phys. Rev. B **83**, 014402 (2011).
[15] V. Pardo and W. E. Pickett, Phys. Rev. Lett. **105**, 266402 (2010).
[16] M. A. Hayward, M. A. Green, M. J. Rosseinsky, and J. Sloan, J. Am. Chem. Soc. **121**, 8843 (1999).
[17] K.-W. Lee and W. E. Pickett, Phys. Rev. B **70**, 165109 (2004).
[18] V. I. Anisimov, D. Bukhvalov, and T. M. Rice, Phys. Rev. B **59**, 7901 (1999).
[19] T. Liu, G. Zhang, X. Zhang, T. Jia, Z. Zeng, and H. Q. Lin, J. Phys.: Condens. Matter **24**, 405502 (2012).
[20] H. Wu, New J. Phys. **15**, 023038 (2013).
[21] N. apRoberts Warren, J. Crocker, A. P. Dioguardi, K. R. Shirer, V. V. Poltavets, M. Greenblatt, P. Klavins, and N. J. Curro, Phys. Rev. B **88**, 075124 (2013).
[22] X.-B. Feng and N. M. Harrison, Phys. Rev. B **69**, 132502 (2004).
[23] K. Schwarz and P. Blaha, Comput. Mater. Sci. **28**, 259 (2003).
[24] J. P. Perdew, K. Burke, and M. Ernzerhof, Phys. Rev. Lett. **77**, 3865 (1996).
[25] A. G. Petukhov, I. I. Mazin, L. Chioncel, and A. I. Lichtenstein, Phys. Rev. B **67**, 153106 (2003).
[26] S. L. Dudarev, G. A. Botton, S. Y. Savrasov, C. J. Humphreys, and A. P. Sutton, Phys. Rev. B **57**, 1505 (1998).
[27] V. Pardo and W. E. Pickett, Phys. Rev. B **85**, 045111 (2012).
[28] J. Fontcuberta, G. Longworth, and J. B. Goodenough, Phys. Rev. B **30**, 6320 (1984).